

Generating single photons at gigahertz modulation-speed using electrically controlled quantum dot microlenses

Cite as: Appl. Phys. Lett. **108**, 021104 (2016); <https://doi.org/10.1063/1.4939658>

Submitted: 30 October 2015 . Accepted: 26 December 2015 . Published Online: 11 January 2016

A. Schlehahn, R. Schmidt, C. Hopfmann, J.-H. Schulze, A. Strittmatter , T. Heindel , L. Gantz, E. R. Schmidgall , D. Gershoni, and S. Reitzenstein 



View Online



Export Citation



CrossMark

ARTICLES YOU MAY BE INTERESTED IN

[Efficient single-photon source based on a deterministically fabricated single quantum dot - microstructure with backside gold mirror](#)

Applied Physics Letters **111**, 011106 (2017); <https://doi.org/10.1063/1.4991389>

[Single-photon emission at a rate of 143 MHz from a deterministic quantum-dot microlens triggered by a mode-locked vertical-external-cavity surface-emitting laser](#)

Applied Physics Letters **107**, 041105 (2015); <https://doi.org/10.1063/1.4927429>

[An electrically driven cavity-enhanced source of indistinguishable photons with 61% overall efficiency](#)

APL Photonics **1**, 011301 (2016); <https://doi.org/10.1063/1.4939831>

Lock-in Amplifiers
up to 600 MHz



Watch



Generating single photons at gigahertz modulation-speed using electrically controlled quantum dot microlenses

A. Schlehahn,¹ R. Schmidt,¹ C. Hopfmann,¹ J.-H. Schulze,¹ A. Strittmatter,^{1,a)} T. Heindel,^{1,b)} L. Gantz,² E. R. Schmidgall,² D. Gershoni,² and S. Reitzenstein¹

¹*Institut für Festkörperphysik, Technische Universität Berlin, 10623 Berlin, Germany*

²*The Physics Department and the Solid State Institute, Technion-Israel Institute of Technology, 32000 Haifa, Israel*

(Received 30 October 2015; accepted 26 December 2015; published online 11 January 2016)

We report on the generation of single-photon pulse trains at a repetition rate of up to 1 GHz. We achieve this speed by modulating the external voltage applied on an electrically contacted quantum dot microlens, which is optically excited by a continuous-wave laser. By modulating the photoluminescence of the quantum dot microlens using a square-wave voltage, single-photon emission is triggered with a response time as short as (281 ± 19) ps, being 6 times faster than the radiative lifetime of (1.75 ± 0.02) ns. This large reduction in the characteristic emission time is enabled by a rapid capacitive gating of emission from the quantum dot, which is placed in the intrinsic region of a p-i-n-junction biased below the onset of electroluminescence. Here, since our circuit acts as a rectifying differentiator, the rising edge of the applied voltage pulses triggers the emission of single photons from the optically excited quantum dot. The non-classical nature of the photon pulse train generated at GHz-speed is proven by intensity autocorrelation measurements with $g^{(2)}(0) = 0.3 \pm 0.1$. Our results combine optical excitation with fast electrical gating and thus show promise for the generation of indistinguishable single photons at rates exceeding the limitations set by the intrinsic radiative lifetime. © 2016 AIP Publishing LLC.

[<http://dx.doi.org/10.1063/1.4939658>]

With the prospect of realizing bright sources of non-classical light on a semiconductor platform,^{1,2} considerable efforts are put into research activities worldwide.^{3,4} In recent years, important steps have been taken, for instance, in the field of quantum communication where single-photon sources based on semiconductor quantum dots (QDs) can act as key building blocks for future technologies.^{5–7} To further optimize efficiency, achievable single-photon rate, and quantum optical quality of the generated photons in terms of high degrees of photon-indistinguishability,⁸ more sophisticated nanophotonic devices with deterministically integrated QDs are promising candidates.^{9,10} However, to achieve maximal repetition rates exceeding the GHz-range,¹¹ a reduction of the lifetime of the QD states—typically ~ 1 ns in case of the InGaAs material system—is required.^{12,13} Exploiting the Purcell effect in the weak coupling regime of micro- or nanocavity structures offers a solution,¹⁴ which, however, inherently suffers from a reduced spectral bandwidth. Alternative approaches to shorten the decay time of QD transitions are to manipulate the state occupation by electrical means. Such implementations accept the probabilistic nature of the emitting device (i.e., some cycles of operation will not result in photon emission), but they are more robust. For example, by applying a reverse bias, charge carriers can be flushed out of the QD¹⁵ or the quantum-confined Stark-effect can be exploited to tune the QD emission fast inside and outside the spectral detection window.¹⁶ Such schemes typically

require sophisticated pulse generators, delivering pulses with widths down to a few 10 ps, most probably hindering a cost-efficient and compact integration of such schemes in the future.

In this work, we present an electrically contacted QD microlens, which, by applying a simple square-wave voltage, converts the emission of a single QD excited by a continuous-wave (CW) laser into a stream of triggered single photons with a characteristic emission decay time much faster than the electrical pulse width itself and also much shorter than the intrinsic radiative lifetime of the QD optical transition. We demonstrate that the emission decay time can be reduced down to (281 ± 19) ps, which corresponds to an improvement by a factor of 6 compared with the emitters' radiative lifetime (1.75 ± 0.02) ns. This allows us to electrically trigger a single-photon pulse-train at 1 GHz repetition rate, even in the absence of cavity quantum electrodynamics effects.

The sample (see Fig. 1(a)) is a p-i-n diode grown via metal-organic chemical vapor deposition (MOCVD) with a low-density layer of InGaAs QDs located in the center of an intrinsic GaAs region. The microlenses are processed by means of 3D electron-beam lithography, here, in contrast to Ref. 9 in a non-deterministic way. After the lithography and etching of 4×4 -arrays of lenses with variable size and shape (cf. Fig. 1(a), inset), a 100-nm-thick planarization layer of hydrogen silsesquioxane (HSQ) is spun onto the sample surface. The HSQ acts as isolation layer between the subsequently deposited semitransparent Ti/Pt contact layer (4/8 nm) and the semiconductor. Finally, to allow for electrical contacting, a large-scale planar Au pad is patterned via

^{a)}Present address: Abteilung für Halbleitertechnik, Otto-von-Guericke Universität, 39106 Magdeburg, Germany.

^{b)}Author to whom correspondence should be addressed. Electronic mail: tobias.heindel@tu-berlin.de

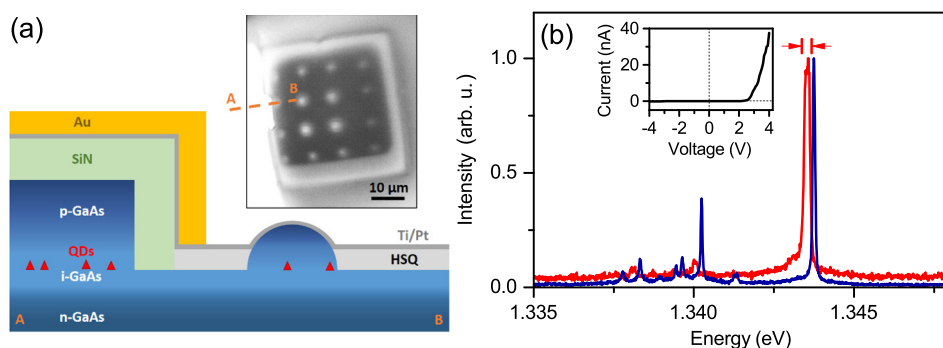


FIG. 1. (a) Schematic cross-section of a p-i-n-doped QD-microlens sample. The microlens is contacted via a planar semitransparent Ti/Pt layer. Inset: Optical microscope image of a microlens array processed using non-deterministic 3D electron-beam lithography. The orange dashed line indicates the cross-section. (b) Electroluminescence spectrum of a single-QD microlens under 200 nA direct current injection (blue line, $T = 20$ K) and electro-optically modulated photo-luminescence spectrum of the same QD under 100 nW optical CW excitation and 1 GHz electrical pulsing at an amplitude of 0.5 V (red line, $T = 20$ K). Red arrows indicate the spectral detection window for time-resolved measurements. Inset: I-V characteristics of the associated 4×4 microlens array.

thermal evaporation. The whole sample is covered with an Au contact at the backside of the n-doped substrate. The sample is mounted inside a He-flow cryostat (20 K) and can be electrically addressed by an integrated micro-probe needle, allowing for convenient contacting the QD-microlenses. In order to electro-optically trigger the emission of single photons, a pulse generator featuring a maximum repetition rate of 3 GHz and variable pulse width, pulse amplitude, and offset is used. QD-microlenses are excited using a CW diode laser emitting at 651 nm. The resulting luminescence is spectrally analyzed by a spectrometer, which comprises a double-grating monochromator and a charge-coupled device camera, enabling a spectral resolution of $25 \mu\text{eV}$. For time-resolved measurements, we use a Si-based single photon counting modules (SPCM) with a timing resolution of 40 ps, which is directly coupled to the side-exit slit of the monochromator using a multi-mode optical fiber. Photon statistics are probed using a fiber-based Hanbury-Brown and Twiss (HBT) setup, comprising a 50:50 beam splitter and two SPCMs with an overall timing resolution of about 380 ps.

The current-voltage (I-V) characteristics of a microlens-array as well as a representative micro-electroluminescence (μEL) spectrum of a microlens containing a single QD under 200 nA direct-current (DC) injection in forward direction are presented in Fig. 1(b), blue line. As expected from the p-n diode design, rectifying behavior with an onset voltage of about 2 V in forward direction is observed. The μEL spectrum shows distinct and narrow emission lines, which, due to the lack of any polarization dependence, are associated with charged QD transitions. Fig. 1(b) shows for comparison also the spectrum of the same QD under optical CW excitation at 100 nW with applied electrical pulses at 1 GHz repetition frequency and an amplitude of 0.5 V (red line). Compared with the spectrum under electrical current injection, the emission line at 1.344 eV shows a linewidth broadening from $78 \mu\text{eV}$ to $196 \mu\text{eV}$, which results from a time-dependent quantum-confined Stark effect.¹⁷ For the time-resolved studies presented in the following, we have chosen the QD emission line marked by red arrows.

Next, the generation of a single-photon pulse-train is pursued, by exploiting the electro-optical excitation introduced above. The time-resolved electro-optically triggered emission of a QD-microlens is presented in Fig. 2. To trigger

the emission of single photons from the CW optically excited QD-microlens, electrical pulses with a width of 8.2 ns, a period of 12.2 ns—corresponding to a rate of 82 MHz—and an adjustable bias offset below the EL onset voltage (~ 2 V) are applied. Such an electrical pulse is indicated in the upper panel of Fig. 2(a). As a reference, constant time-resolved PL (TRPL) emission under CW laser excitation at flat-band condition ($V_{\text{bias}} = 2$ V) without applied electrical pulses is shown (cf. Fig. 2(a), grey curve). In the following, the pulse amplitude ΔV of the applied voltage is varied between 0 V (no pulses) and 1.1 V, by varying the bias voltage and fixing the maximum voltage level at +1 V (cf. Fig. 2(a), upper panel). Under such electro-optical excitation conditions, we observe a pronounced pulsed emission triggered by the rising edge of the electrical pulse, while emission is effectively quenched otherwise. Remarkably, even an amplitude ΔV as small as 0.1 V (blue line) is sufficient to trigger emission from the QD-microlens. Moreover, the optical pulse width depends on the electrical pulse amplitude, which allows for a reduction of the FWHM from (1.96 ± 0.16) ns at 0.1 V amplitude (Fig. 2(a), blue line) to (0.88 ± 0.03) ns at 1.1 V (Fig. 2(a), black line). On the other hand, by increasing ΔV from 0.1 V to 1.1 V, we observe a reduction in emission intensity of the QD state of 50%. Based on the detected count rates at the SPCMs and a measurement of the setup efficiency, we estimate a photon extraction efficiency of the present device of about 1%. We expect this efficiency to be greatly improved in future, by utilizing deterministic device approaches combined with a mirror beneath the QDs⁹ and transparent top contacts made out of indium-tin-oxide. In order to prove that the emission is indeed electro-optically triggered, rather than pulsed electroluminescence, two reference measurements without any optical excitation were performed for the smallest and largest amplitude (see Fig. 2(a)), resulting in no detectable signal. The fast periodic triggering of the emitter's emission can be explained in terms of an abrupt depletion and refilling of the QD states via a fast tilt of the band structure (cf. Fig. 2(b), insets), while the pulsed emission arises from a differentiating character of the device, which is attributed to its voltage dependent junction capacitance $C_J(\Delta V) = A[(e\epsilon N_A N_D)/(2(N_A + N_D)(V_{\text{bi}} + \alpha\Delta V))]^{1/2}$ connected in series with a resistance R_S of the whole circuit, including, e.g., the serial resistance of the contacts (cf. equivalent circuit in

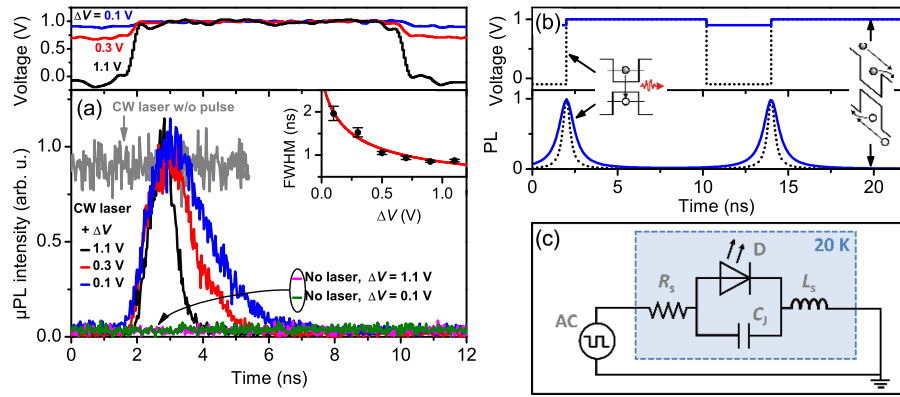


FIG. 2. (a) Time-resolved photoluminescence from an electro-optically controlled QD-microlens, for various amplitudes of the electrical pulse. The applied electrical pulses (8.2 ns long, at a repetition rate of 82 MHz), monitored by an oscilloscope, with amplitude ΔV and bias offset V_{bias} are shown in the upper panel. The inset displays the resulting full width at half maximum (FWHM) of the emitted light pulse as a function of the pulse amplitude ΔV (black circles) together with a model-fit (red line), which considers the differentiating character of our device in combination with a ΔV dependent junction capacitance $C_J(\Delta V)$. (b) Schematic of the externally applied electrical pulse pattern (upper panel) and resulting photoluminescence (PL) due to charge-carrier transport through the QD layer for two different pulse amplitudes. Inset: Schematic of the band-structure of a QD in the intrinsic region. (c) Equivalent circuit of our device acting as a built-in rectifying differentiator (abbreviations: square-wave voltage source (AC), p-i-n diode (D), junction capacitance (C_J), serial resistance (R_S), serial inductivity (L_S)).

Fig. 2(c)). Here, A denotes the device area, e is the elementary charge, $\epsilon = \epsilon_r \epsilon_0$ is the permittivity of the material arising from the product of the relative and vacuum permittivity, N_A and N_D are the doping concentration of the p- and n-doped regions of the diode ($N_A = 1.2 \times 10^{19} \text{ cm}^{-3}$ and $N_D = 3.0 \times 10^{18} \text{ cm}^{-3}$), and V_{bi} is the built-in voltage of the junction ($V_{\text{bi}} \approx 1.4 \text{ eV}$). For a full description of the dynamics, we also need to take into account a parasitic inductivity L_S which effectively leads to characteristic resonance frequencies of our RCL-circuit. On resonance, e.g., at the chosen frequency of 82 MHz, the voltage at the p-i-n-junction is enhanced, which we consider by the factor α . Good agreement with the experimental data in Fig. 2(a) (inset) was obtained for $\alpha = (14 \pm 5)$. This multiplication factor can also explain that voltage variations as low as $\Delta V = 0.1 \text{ V}$ are sufficient to trigger emission of light in our device. As the p-i-n junction is biased below the onset of EL, the optically generated charge-carriers are continuously expelled from the active area due to tunneling, which is effectively suppressed at the rising edge of the applied pulse. The FWHMs

presented in Fig. 2(a) are, therefore, directly related to the voltage dependence of the time constant τ of the differentiator circuit: $\tau(\Delta V) = R_S C_J(\Delta V)$. The fact that only the rising edge of the electrical pulse gates the emission of light is attributed to the rectifying character of the diode. Figs. 2(b) and 2(c) illustrate this behavior and the associated equivalent circuit. We would like to stress that the presented trigger scheme, based on a built-in differentiation mechanism, might be very beneficial for practical non-classical light sources, as it does not require an external driver delivering ultra-short voltage pulses. It is also noteworthy that in contrast to results obtained in Ref. 18, we observe no background emission in between the optical pulses for a sufficiently large amplitude, which can be an important advantage for, e.g., applications requiring ultra-low background light-levels in pulsed experiments.

The specific trigger mechanism observed in our QD-microlenses enables the QD to emit optical pulse trains in the GHz regime, which is demonstrated in the lower panel of Fig. 3(a). The observed pulse trains electro-optically

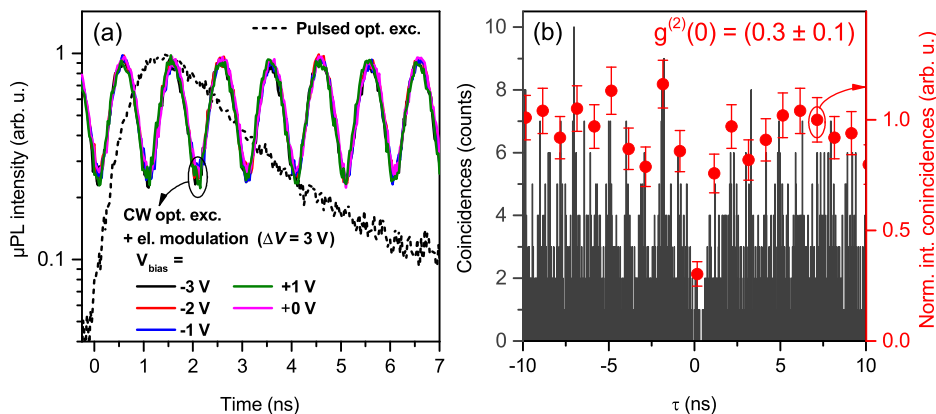


FIG. 3. (a) Time-resolved photoluminescence emission resulting from single-QD exciton recombination under CW optical excitation with electrical modulation at 1 GHz repetition rate for various bias voltages V_{bias} at constant pulse amplitude. The μPL resulting from pulsed optical excitation without electrical pulsing is displayed for reference (dashed line). The photoluminescence signal duration is reduced by a factor of 6 due to electrical depletion. (b) Photon-autocorrelation measurement of the photoluminescence under electrical modulation at 1 GHz ($V_{\text{bias}} = 0 \text{ V}$ and $\Delta V = 3 \text{ V}$). The histogram displays the raw data, whereas filled circles correspond to the same data with a time-bin width of 1 ns equal to the electrical pulse period. A $g^{(2)}(0)$ value of 0.3 ± 0.1 is obtained.

triggered at 1 GHz were recorded for various bias voltages between -3 V and $+1\text{ V}$ at a constant amplitude of $\Delta V = 3\text{ V}$, revealing that the quenching is not noticeably influenced by the offset within the limits of the pulse generator. This insensitivity of the bias voltage at a given amplitude further supports the assumption of an emission gating by a differentiated pulse. The repetition rate of triggered QD single-photon sources is usually limited by the radiative emission lifetime of the respective excited state, and can, e.g., be enhanced by means of the Purcell effect in QD-microcavity structures.²⁰ To illustrate this aspect for the present system, TRPL measurements were performed at a pulse repetition rate of 82 MHz without any electrical modulation at zero bias voltage. The corresponding PL transient is presented in Fig. 3(a) as a reference (dashed line). This trace is compared with the CW excited and electrically modulated emission at 1 GHz. From the TRPL data, we extract a radiative emission lifetime of $(1.75 \pm 0.02)\text{ ns}$, whereas the electro-optically modulated signal shows a decay time of $(281 \pm 19)\text{ ps}$, which corresponds to a reduction by a factor of 6. Thus, in the present device design, a significant enhancement of the maximal achievable repetition rate well above the radiative-lifetime-limited rate can be obtained without the need for complex microcavity structures or sophisticated electronic pulse shaping. A possible application for this operation scheme is to realize a fast resonantly excited source of indistinguishable photons, which can be operated with standard CW tunable lasers and spectral post-selection.¹⁹ In contrast, to achieve high degrees of photon-indistinguishability using standard current injection schemes is challenging, due to the intrinsic time jitter and electric field noise associated with above-band excitation.

As a proof-of-concept, an off-resonantly driven single-photon source operated at 1 GHz is demonstrated in Fig. 3(b). In order to prove the non-classical statistics of the light emitted within this fast optical pulse train, photon-autocorrelation measurements were performed using the fiber-coupled HBT setup. The corresponding coincidence histogram recorded under electro-optical excitation with 3 V pulse amplitude and a bias voltage of 0 V is shown in Fig. 3(b). Setting the time-bin-width (1 ns) to the inverse modulation speed reveals a $g^{(2)}(0)$ -value of 0.3 ± 0.1 (red points), clearly demonstrating single-photon emission at a repetition rate of 1 GHz. This represents a promising starting point towards more sophisticated single-photon devices. For instance, since we use a planar semi-transparent metal layer to electrically address the microlenses, our contacting scheme can be easily combined with 3D *in-situ* cathodoluminescence-lithography techniques reported in Ref. 9. These techniques can be applied to fabricate deterministic electrically controlled single-QD microlenses with enhanced photon extraction efficiency. In combination with resonant excitation schemes,¹⁹ this method becomes a powerful quantum device concept for the realization of efficient, ultra-fast sources of indistinguishable photons, and might even be completely integrated on-chip.²¹ On the other hand, the fast electrically controlled depletion of QD charge-carriers observed in Fig. 3(a) is also desirable for spin-control experiments using dark exciton states²² and can increase the state-preparation-fidelity compared with optical depletion schemes used so far.²³

In summary, we presented fast electro-optical triggering of single photons from an electrically contacted QD-microlens. Our scheme makes use of fast electric field switching effects in order to overcome limitations on the single-photon pulse-train generation, set by the intrinsic exciton lifetime. The electrical operation scheme exploits a built-in differentiation mechanism of the QD-microlens to trigger the emission of single photons, which dispenses the need for an external driver delivering ultra-short voltage pulses. This appealing feature allowed us to transform an off-resonantly excited, CW photoluminescence signal from a QD-confined exciton into a train of sub-nanosecond optical pulses, triggered by the rising edge of the applied square-wave voltage, where the optical pulse width is controlled by the voltage amplitude. The edge-triggering scheme leads to a reduction in the decay times of the optical pulses down to $(281 \pm 19)\text{ ps}$, a factor of 6 in comparison with the intrinsic lifetime $(1.75 \pm 0.02)\text{ ns}$ of the QD. It also enables the generation of single photons with $g^{(2)}(0) = 0.3 \pm 0.1$ up to a repetition rate of 1 GHz. Thus, our electrically contacted QD-microlenses may operate as source of indistinguishable photons, operating in the GHz regime.

This work was financially supported by the German-Israeli Foundation for Scientific Research and Development (GIF, Grant No. 1148-77.14/2011), the German Federal Ministry of Education and Research (BMBF) through the VIP-project QSOURCE (Grant No. 03V0630), and the German Research Foundation (DFG) within the Collaborative Research Center SFB 787 “Semiconductor Nanophotonics: Materials, Models, Devices.”

¹E. Dekel, D. Gershoni, E. Ehrenfreund, J. M. Garcia, and P. M. Petroff, *Phys. Rev. B* **61**, 11009 (2000).

²P. Michler, A. Kiraz, C. Becher, W. V. Schoenfeld, P. M. Petroff, L. Zhang, E. Hu, and A. Imamoglu, *Science* **290**, 2282 (2000).

³G.-C. Shan, Z.-Q. Yin, C. H. Shek, and W. Huang, *Front. Phys.* **9**, 170 (2014).

⁴N. Gregersen, P. Kaer, and J. Mørk, *IEEE J. Sel. Top. Quantum Electron.* **19**, 9000516 (2013).

⁵E. Waks, K. Inoue, C. Santori, D. Fattal, J. Vuckovic, G. S. Solomon, and Y. Yamamoto, *Nature* **420**, 762 (2002).

⁶T. Heindel, C. A. Kessler, M. Rau, C. Schneider, M. Fürst, F. Hargart, W.-M. Schulz, M. Eichfelder, R. Roßbach, S. Nauerth, M. Lerner, H. Weier, M. Jetter, M. Kamp, S. Reitzenstein, S. Höfling, P. Michler, H. Weinfurter, and A. Forchel, *New J. Phys.* **14**, 083001 (2012).

⁷M. Rau, T. Heindel, S. Unsleber, T. Braun, J. Fischer, S. Frick, S. Nauerth, C. Schneider, G. Vest, S. Reitzenstein, M. Kamp, A. Forchel, S. Höfling, and H. Weinfurter, *New J. Phys.* **16**, 043003 (2014).

⁸C. Santori, D. Fattal, J. Vučković, G. S. Solomon, and Y. Yamamoto, *Nature* **419**, 594 (2002).

⁹M. Gschrey, A. Thoma, P. Schnauber, M. Seifried, R. Schmidt, B. Wohlfeil, L. Krüger, J. H. Schulze, T. Heindel, S. Burger, F. Schmidt, A. Strittmatter, S. Rodt, and S. Reitzenstein, *Nat. Commun.* **6**, 7662 (2015).

¹⁰L. Sapienza, M. Davanço, A. Badolato, and K. Srinivasan, *Nat. Commun.* **6**, 7833 (2015).

¹¹E. Stock, W. Unrau, A. Lochmann, J. A. Töfflinger, M. Öztürk, A. I. Toropov, A. K. Bakarov, V. A. Haisler, and D. Bimberg, *Semicond. Sci. Technol.* **26**, 014003 (2011).

¹²D. J. P. Ellis, P. Atkinson, P. See, M. B. Ward, R. M. Stevenson, Z. L. Yuan, D. C. Unitt, D. J. P. Ellis, K. Cooper, D. A. Ritchie, and A. J. Shields, *New J. Phys.* **10**, 043035 (2008).

¹³A. Schlehahn, M. Gaafar, M. Vaupel, M. Gschrey, P. Schnauber, J.-H. Schulze, S. Rodt, A. Strittmatter, W. Stolz, A. Rahimi-Iman, T. Heindel, M. Koch, and S. Reitzenstein, *Appl. Phys. Lett.* **107**, 041105 (2015).

¹⁴J.-M. Gérard, B. Sermage, B. Gayral, B. Legrand, E. Costard, and V. Thierry-Mieg, *Phys. Rev. Lett.* **81**, 1110 (1998).

- ¹⁵F. Hargart, C. A. Kessler, T. Schwarzbäck, E. Koroknay, S. Weidenfeld, M. Jetter, and P. Michler, *Appl. Phys. Lett.* **102**, 011126 (2013).
- ¹⁶A. Bennett, R. B. Patel, A. J. Shields, K. Cooper, P. Atkinson, C. A. Nicoll, and D. A. Ritchie, *Appl. Phys. Lett.* **92**, 193503 (2008).
- ¹⁷S. A. Empedocles and M. G. Bawendi, *Science* **278**, 2114 (1997).
- ¹⁸M. Jijang, Y. Kumamoto, A. Ishii, M. Yoshida, T. Shimada, and Y. Kato, *Nat. Commun.* **6**, 6335 (2015).
- ¹⁹Y. Cao, A. J. Bennett, D. J. P. Ellis, I. Farrer, D. A. Ritchie, and A. J. Shields, *Appl. Phys. Lett.* **105**, 051112 (2014).
- ²⁰T. Heindel, C. Schneider, M. Lermer, S. H. Kwon, T. Braun, S. Reitzenstein, S. Höfling, M. Kamp, and A. Forchel, *Appl. Phys. Lett.* **96**, 011107 (2010).
- ²¹P. Munnely, T. Heindel, M. M. Karow, S. Höfling, M. Kamp, C. Schneider, and S. Reitzenstein, *IEEE J. Sel. Top. Quantum Electron.* **21**, 1900609 (2015).
- ²²I. Schwartz, E. R. Schmidgall, L. Gantz, D. Cogan, E. Bordo, Y. Don, M. Zielinski, and D. Gershoni, *Phys. Rev. X* **5**, 011009 (2015).
- ²³E. R. Schmidgall, I. Schwartz, D. Cogan, L. Gantz, T. Heindel, S. Reitzenstein, and D. Gershoni, *Appl. Phys. Lett.* **106**, 193101 (2015).